

Rotamers and Isomers in the Fulgide Series. Part 1. Stereochemistry and Conformational Analysis of Bis-(3,4-dimethoxybenzylidene)succinic Anhydrides by X-Ray Crystallography and Molecular Mechanics

Jan C. A. Boeyens,* Louis Denner, and Guido W. Perold

Department of Chemistry, University of the Witwatersrand, Wits, 2050 South Africa

Conformational analysis of bis-(3,4-dimethoxybenzylidene)succinic anhydride suggests that in addition to a *Z,Z*-isomer, the *E,E*-isomer of this diarylfulgide occurs as three distinct relatively freely interconvertible chiral rotamers and their enantiomers. The *E,Z*-isomer undergoes facile dehydrogenation to form an aryl naphthalene derivative. Crystals were obtained of a symmetrical *E,E*-rotamer in two forms, the *Z,Z*-isomer and the aryl naphthalene derivative. X-Ray structures of these crystalline forms are reported. The conformations of the other rotamers were simulated by molecular mechanics, using an empirical force-field based on the observed structure of the symmetrical *E,E*-rotamer, described here. The aromatic rings of the *E,E*-isomers are eclipsed and under severe strain, which inhibits free rotation. Packing energy promotes the crystallization of one of the possible *E,E*-rotamers only and has a marked effect on the orientation of the methoxy substituents.

The fulgides¹ (dimethylenesuccinic anhydrides or 3,4-dimethylenedihydrofuran-2,5-diones) are typically highly crystalline compounds which in many cases are thermochromic² and phototropic.³⁻⁵ In the case of *E,E*-diarylfulgides such as (1) they can undergo dehydrogenation on irradiation or on strong

heating to afford 1-arylnaphthalene-2,3-dicarboxylic anhydrides (4). This sequence has been long and fruitfully studied⁶ and has been shown⁶ to involve isomerization to an *E,Z*-isomer (2) followed by thermal disrotatory and photochemical conrotatory changes leading *via* 1,5-H shifts to 1,2-dihydro-naphthalene intermediates such as (3). In the case of (*E,E*)-bis-(*p*-methoxybenzylidene)succinic anhydride, irradiation has been reported⁷ to afford both the *E,Z*- and *Z,Z*-isomers, and we found⁸ that rotameric isomerism can occur in the case of the *E,E*-isomer.

For the known bis-(3,4-dimethoxybenzylidene)succinic anhydride [1; R = 3,4-(MeO)₂]⁹ we found¹⁰ that the additional chemical activation due to the methoxy groups leads to ready formation of the naphthalene anhydride [4; R = 3,4-(MeO)₂] by either warming (1) in solution, or chromatographing it over silica gel. We could now arrive at the exact description of this molecule by X-ray diffraction analysis (below). In the same manner we were able to demonstrate the *E,E*-configuration of anhydride [1; R = 3,4-(MeO)₂] and also the orientation of the methoxy groups as shown (6). The formation of the naphthalenedicarboxylic anhydride (4) involves isomerization of one double bond of (1). We found that under the mild conditions for these changes, isomerization of both double bonds also occurs to afford the *Z,Z*-anhydride (5) in low yield as deep orange needles, m.p. 205–207 °C. This behaviour is in contrast with that of other diarylfulgides where irradiation or strong heating is required to effect such changes.⁷

X-Ray diffraction analysis of the *Z,Z*-isomer (5) afforded its structure and showed that the planes of the carbonyl groups and adjacent aromatic rings are nearly parallel. Delocalization of the π -systems of these groups is therefore favoured and this can explain the very intense long-wave absorption of this isomer, relative to the *E,E*-isomer (6) [λ (ϵ) (CHCl₃-EtOH, 1:1 v/v) for (6): 441 nm (12 000) and 326 nm (16 000); for (5): 446 nm (20 000) and 345 nm (15 000)]. The auxochromic shift is thus for the transition from *E,E* to *Z,Z*, as opposed to the auxochromic shift normally expected.¹¹ We have encountered this effect also in the case of 3,4-dimethoxybenzylidenesuccinic anhydride¹² and it has been reported for the case of *p*-methoxybenzylidenesuccinic anhydride.¹³

The n.m.r. characteristics of these fulgides reflect the differences arising from the relationships between the aromatic

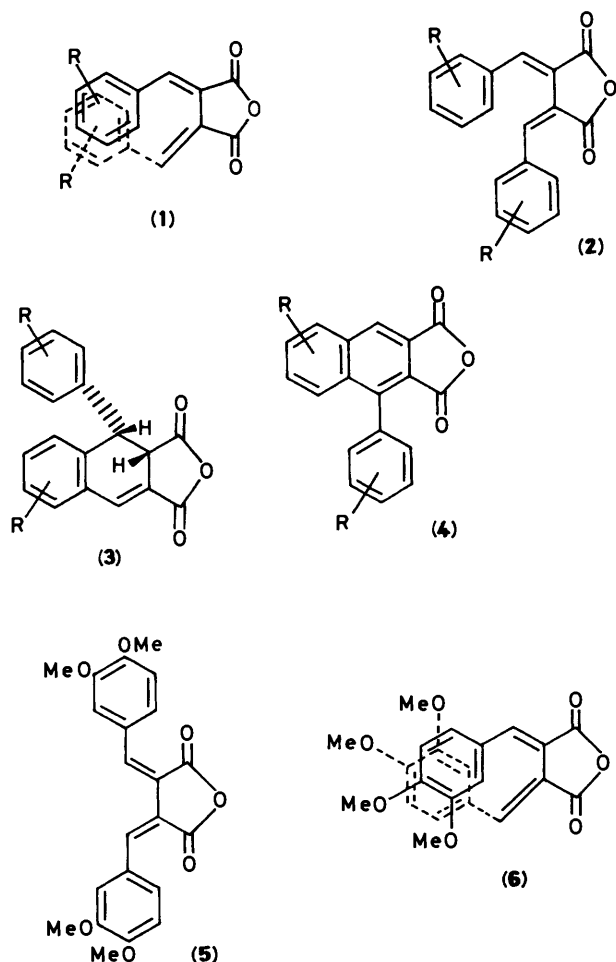
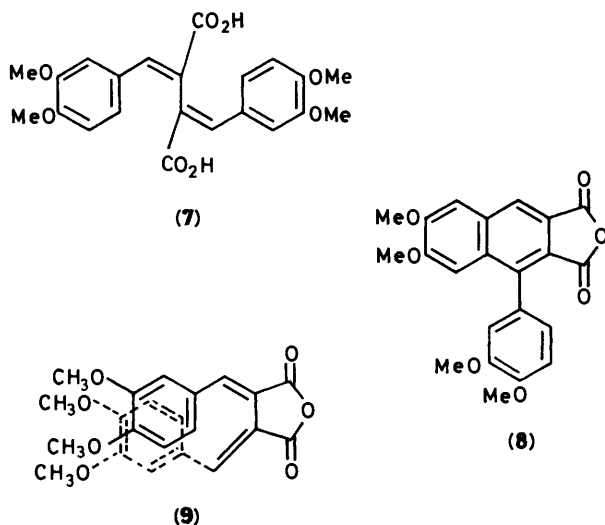


Table 1. Semiquantitative ratios of summed intensities of methoxy nuclear magnetic resonances^a of the isomeric anhydrides in CDCl₃ solution at 200 MHz (Bruker AC 200 FT spectrometer)

Products	Starting from <i>E,E</i> -isomer (6)				Starting from <i>Z,Z</i> -isomer (5)					
	<i>E,E</i>	<i>x</i>	<i>y</i>	<i>w</i>	<i>Z,Z</i>	<i>E,E</i>	<i>x</i>	<i>y</i>	<i>w</i>	<i>Z,Z</i>
Conditions										
Fresh solution	100									100
Degassed solution										
kept 1 h/24 °C	74	11	12	—	3					
kept 3 h/24 °C						2	17	21	—	60
kept 3 h/73 °C						15	28	32	—	25
kept 5 h/73 °C	28	28	28	3	14					
kept 11 h/73 °C	24	24	27	10	15	27	26	27	4	17

^a For *E,E* at 3.85 and 3.55; for *x* at 3.95 and 3.79; for *y* at δ 3.972 and 3.966; for *w* at 3.92 and 3.76; for *Z,Z* at 4.01 and 3.99.



rings in the *E,E*-isomer, and between the aromatic ring and the adjacent carbonyl group in the *Z,Z*-isomer. In the *E,E*-situation (6) the three aromatic proton resonances are close together at δ 6.7, 6.5, and 6.5¹⁰ while in the *Z,Z*-isomer they are widely spread at δ 8.2, 7.5, and 6.9 due to the anisotropic effect of the carbonyl group. This characteristic differentiation is also encountered for 3,4-dimethoxy-¹² and *p*-methoxybenzylidene-succinic anhydrides.¹³

The resonances of the methoxy groups differ markedly from each other for the *E,E*-isomer (δ 3.85 and 3.55), while they are close together for the *Z,Z*-isomer (δ 4.01 and 3.99). This peculiarity can be used to follow the isomerization of the *E,E*- and the *Z,Z*-isomers in detail.

Freshly prepared solutions of the *E,E*- and the *Z,Z*-anhydrides (6) and (5) in CDCl₃ gave clean n.m.r. spectra; each of these solutions was then degassed by repeated cycles of freezing in liquid nitrogen followed by thawing and then sealed at 0.05 Torr. The changing composition of the mixtures was followed during a heating program by the summation of the two methoxy group intensities for each isomer. New peaks in this region appeared in time as a spread pair at δ 3.95 and 3.79 (= *x*) and as a close pair at δ 3.972 and 3.966 (= *y*); at the same time a new set of 1,2,4-trisubstituted aromatic proton signals appeared at δ 7.29 (d, *J* 2 Hz), 7.16 (dd, *J* 2 and 8 Hz), and 6.85 (d, *J* 8 Hz), as also two olefinic proton signals of equal intensity at δ 7.99 and 7.65. After longer times and higher temperatures another

spread pair of singlets appeared at δ 3.92 and 3.76 (= *w*). These results are in Table 1 and are regarded as semiquantitative and indicative. The *E,E*- and *Z,Z*-anhydrides thus move into equilibrium with each other to give the same mixture from either side.

The (*y*) pair of methoxy group resonances may be ascribed to the methoxy groups on an aromatic ring close to a carbonyl group, and the (*x*) pair of signals to methoxy groups on an aromatic ring overlaying another centre of anisotropy such as a double bond or another aromatic ring. Table 1 furthermore shows that the concentrations of the (*x*) and the (*y*) species effectively remain equal at all levels. They may therefore be jointly ascribed to the *E,Z*-anhydride [2; R = 3,4-(MeO)₂]. We can, therefore, follow the formation of the *E,Z*-anhydride in oxygen-free solution. On long continued runs a superimposed doublet of doublets centred at δ 5.0 (*J ca.* 5 Hz) emerged. Such resonances have been found for a dihydronaphthalene intermediates such as (3).⁶

This equilibration was carried out on the preparative scale starting with pure *E,E*-anhydride (6). After prolonged heating (see Experimental section) the mixture was worked up in the normal manner with exposure to air. As in an earlier report¹⁰ the main product isolated was the aromatized naphthalene anhydride [4; R = 3,4-(MeO)₂].

The further isomer (*w*) that appears on continued heating, with its methoxy group resonances as a spread pair at δ /3.92 and 3.76 could then have a 3,4-dimethoxyphenyl ring overlaying another aromatic ring, as in the *E,E*-anhydride (6). We have investigated the possibility of the separate existence of rotamers of the *E,E*-anhydride (6) and we demonstrate (below) that a molecular energy minimum for such a rotamer can be found by calculation. We therefore ascribe this pair of methoxy group resonances to a rotamer such as (9).

Change of solvent had a marked effect on the equilibration of the *E,E*- and *Z,Z*-anhydrides. Thus anhydride (6) kept for 11 days in acetonitrile solution at 60 °C gave 68% recovery, on crystallization from acetonitrile, of a solvated form of (6) as pure yellow flat needles, m.p. *ca.* 100 °C while changing to the unsolvated form which crystallized on the hot-stage and then finally melted at 174 °C as for the latter. These crystals were satisfactory for X-ray analysis which demonstrated the *E,E*-configuration of the solvated molecules in the crystal. Fractional crystallization of the mother liquor afforded the *Z,Z*-anhydride (5) in low yield (4%).

Irradiation at 366 nm of the *E,E*-anhydride (6) in acetone solution gave recovery of the naphthalenedicarboxylic anhydride [4; R = 3,4-(MeO)₂] in 14% yield. When the parent fulgenic acid (7) was similarly irradiated it showed, by silylation/g.l.c. analysis, part conversion into products with less volatile silyl esters: for the starting material, ET₁₉₇ 269 °C (99%), and for the product mixture, ET₁₉₇ 269 °C (73%) and ET₁₉₇ 274 °C (25%). Chromatography of the recovered mixture over silica gel gave major fractions (72%) with constituents at ET₁₉₇ 269 °C (68%) and ET₁₉₇ 274 °C (26%). Cyclization with acetyl chloride and fractional crystallization of the product afforded only the *Z,Z*-anhydride (5) in 8% yield overall.

When the fulgenic acid (7) was irradiated as above for 24 h, and the product dehydrated as before, only the dehydrogenated naphthalenedicarboxylic anhydride [4; R = 3,4-(MeO)₂] could be obtained in crystalline form in 19% yield.

Experimental

Measurements routinely involved Kofler micro hot-stage (m.p.), Pye Unicam SP300 (i.r. for dispersions in KBr), Unicam SP1800 (u.v.-vis), Varian-MAT CH7 (m.s.), Bruker WP 80 MHz FT spectrometer (n.m.r. in deuteriochloroform solutions), and Pye Unicam GCD chromatograph (g.l.c.). T.l.c. was on pre-

coated silica gel plates (Merck F254). Analytical g.l.c. was over a column (1.4 × 0.0026 m) of OV17 (1% on Anakrom Q) with nitrogen as carrier gas at 24 ml min⁻¹, all runs were programmed at 8 °C min⁻¹, injector and detector ports were at 300 °C, and emergent peak temperatures (ET) were read from the oven temperature and are recorded as ET (starting temperature in °C). Approximate product distributions were calculated on peak heights.¹⁴ Irradiation at 366 nm was done with a medium-pressure mercury lamp (Applied Photophysics model 3 010, 125 W) used in a water-cooled Pyrex well.

Bis-(3,4-dimethoxybenzylidene)succinic Acid (7).—This compound was prepared by slow addition of diethyl succinate (1 mol) and veratraldehyde (2 mol) together in toluene solution to a stirred suspension of sodium hydride (2 mol) in toluene. The crude acids in acetonitrile afforded the less soluble diacid (7) which was leached out four times with hot butanone to give fine yellow grains, m.p. 213–216 °C (decomp.). [lit.,⁹ 220 °C (decomp.)], purity by silylation/g.l.c. 99%, ET₁₉₇ 269 °C, in 25% recovery. Its anhydride (6) had m.p. 173 °C^{9,10} and slow crystallization from acetone solution afforded ruby hexagonal prisms which were suitable for X-ray diffraction studies. This established structure (6) in detail and confirmed the *E,E*-configuration.

(Z,Z)-Bis-(3,4-dimethoxybenzylidene)succinic Anhydride (5).—This compound was obtained by keeping the *E,E*-anhydride (6)⁹ (50 mg) in acetone (5 ml) on silica gel (2 g) for 16 h at 25 °C. The product was washed out with acetone (30 ml) through a small bed of silica gel. It was obtained as an orange gum (44 mg) from acetone (0.4 ml) and then from acetonitrile–dimethylformamide (5:1 v/v) to give the *Z,Z*-anhydride (5), m.p. 205–207 °C (3 mg). It was repeatedly recovered by chromatography of the crude products from different runs over silica gel in benzene–acetic acid (9:1 v/v) and by crystallizing combined (t.l.c.) fractions as above (*M*⁺ Found: 396.124; C₂₂H₂₀O₇ requires 396.121); λ_{max}. (CHCl₃–EtOH, 1:1 v/v) 446 (ε 20 000) and 345 nm (15 000); ν_{max}. 1 825, 1 790 and 1 765 (C=O), and 1 020 cm⁻¹ (C–O–C); δ (250 MHz) 8.25 (2 H, d, *J* 2 Hz, ArH), 7.51 (2 H, dd, *J* 2 and 8 Hz, ArH), 7.35 (2 H, s, olefinic), 6.95 (2 H, d, *J* 9 Hz, ArH), 4.01 (6 H, s, OMe), and 3.99 (6 H, s, OMe); *m/z* 396 (*M*⁺, 100%) and 138 (66%). A fresh 1% solution of anhydride (5) in dimethylformamide on g.l.c. showed major components at ET₂₃₈ 279 °C (20%) and 305 °C (75%) while after 2 h at 102 °C it showed peaks at ET₂₃₈ 279 °C (5%) and 305 °C (92%) as for anhydride (6).¹⁰

6,7-Dimethoxy-1-(3,4-dimethoxyphenyl)naphthalene-2,3-dicarboxylic Anhydride [4; R = 3,4-(MeO)₂] from Anhydride (5).—(a) Anhydride (5) (104 mg crude) in acetone (3 ml) was dried on silica gel (1.5 g). The free-flowing powder was kept in a flask stoppered with cotton wool for 19 h at 52 °C, loaded onto a column of silica gel (40 g), and chromatographed in benzene–acetic acid (9:1 v/v). Front running fractions (42 mg) yielded unchanged anhydride (5) (5 mg), flat orange needles as before; δ (80 MHz) 8.23 (2 H, d, *J* 2 Hz), 7.50 (2 H, dd, *J* 2 and 8 Hz), 7.34 (2 H, s), 6.93 (2 H, d, *J* 9 Hz), 4.00 (6 H, s), and 3.97 (6 H, s); *m/z* 396 (*M*⁺, 100%) and 138 (94). Later fractions (40 mg) from acetone afforded the naphthalenedicarboxylic anhydride [4; R = 3,4-(MeO)₂] as micro-crystalline grains (9 mg), m.p. 317 °C after recrystallization in rhombs on the hot stage around 300 °C, and identical with the product reported earlier.¹⁰

(b) Anhydride (5) (5 mg) and acetonitrile (0.3 ml) were sealed in a tube under nitrogen at 0.5 Torr. On quickly warming the intensely orange solution, its colour changed to a light lemon shade at 170 °C. After brief heating to 250 °C and then cooling, glistening microscopic rhombs of the naphthalenedicarboxylic anhydride [4; R = 3,4-(MeO)₂] (3 mg) were deposited,

m.p. 315–317 °C as above, with i.r. absorption and m.s. identical with that of the earlier preparation. The characteristic m.p. behaviour of this compound had been noted before¹⁵ and was observed in all preparations of it.

The anhydride [4; R = 3,4-(MeO)₂] was always obtained as light coloured grains or small scales. A single crystal for X-ray diffraction analysis was obtained by sealing it (1 mg) in a Pyrex tube together with acetonitrile (100 μl) and dimethylformamide (2 μl), heating once to 200 °C, and then subjecting it to repeated cycles of heating to 80 °C followed by slow cooling to room temperature over a period of 17 days. The crystals were then fairly substantial platelets.

Preparative Isomerization of E,E-Bis-(3,4-dimethoxybenzylidene)succinic Anhydride (6) in Solution.—The *E,E*-anhydride (6) (402 mg) in chloroform (10 ml) in a stout-walled tube was degassed by cycles of freezing in liquid nitrogen at 0.05 Torr followed by thawing. After sealing it was heated at 73 °C for 7 h. The product recovered on evaporation was dissolved in acetonitrile (10 ml), degassed as before, and the sealed tube heated at 103 °C for 88 h. The dried product heated in acetone (3 ml) gave yellow grains (101 mg) of the substituted naphthalene anhydride [4; R = 3,4-(MeO)₂], m.p. 314–316 °C and behaviour as before.

Solvated E,E-Anhydride (6).—The *E,E*-anhydride (6) (304 mg) in acetonitrile (15 ml) was heated, with limited access of air, at 60 °C for 11 days. The solvent was evaporated off until 4 ml remained; yellow pointed needles crystallized (207 mg), which on two-fold recrystallization from acetonitrile did not change, m.p. ca. 100 °C, and solidified to the unsolvated form as red plates which finally melted at 174 °C. These crystals were suitable for X-ray work and were thus shown to have an unchanged *E,E*-configuration.

Fractional crystallization of the foregoing mother liquor from acetonitrile gave a low yield of the *Z,Z*-anhydride (5) (11 mg, 3%), m.p. 202–206 °C; δ 8.23 (d, *J* 2 Hz), 7.50 (dd, *J* 2 and 8 Hz), 7.33 (s), 6.93 (d, *J* 8 Hz), 3.99 (s) and 3.97 (s) as before.

Irradiation of the E,E-Anhydride (6).—The *E,E*-anhydride (6) (403 mg) in acetone (50 ml) was irradiated at 366 nm for 6 h. Concentration of the solution afforded the naphthalenedicarboxylic anhydride [4; R = 3,4-(MeO)₂] (57 mg 14%), m.p. 308–312 °C and behaviour as before.

Irradiation of Fulgenic Acid (7) at 366 nm.—(a) For 3 h. Fulgenic acid (7) (400 mg) in acetone (50 ml) was irradiated for 3 h, when the starting material with ET₁₉₇ 268 °C (99%) had changed to a mixture of acids with ET₁₉₇ 269 °C (73%) and with ET₁₉₇ 274 °C (25%). This mixture was spread on silica gel (2.2 g) and chromatographed over silica gel (100 g) in benzene–ethyl acetate–acetic acid (8:5:1, v/v). Major fractions (286 mg) analysed for ET₁₉₇ 269 °C (68%) and ET₁₉₇ 274 °C (26%) and this mixture was cyclized with acetyl chloride (5.5 ml) for 3 h at 53 °C. The recovered product fractionally crystallized from acetone and then from acetonitrile finally gave the *Z,Z*-anhydride (5) in 8% yield.

(b) For 24 h. Fulgenic acid (7) (406 mg) in acetone (50 ml) was irradiated at 366 nm for 24 h and the recovered mixture treated with acetyl chloride (8 ml) for 30 h at 50 °C and crystallized from acetone to afford the naphthalenedicarboxylic anhydride [4; R = 3,4-(MeO)₂] (64 mg, 19%), m.p. 312–314 °C as before, as the only crystallizable product recovered.

Crystal Data.—Single crystals were examined by standard optical and photographic X-ray methods. Crystals of (6),^{9,10} m.p. 173.5 °C (lit.,⁹ 172–173 °C), were obtained as well-developed ruby hexagonal prisms on slow evaporation of its

Table 2. Crystal data and details of the crystallographic analyses

Compound	(6)	(5)	(8)	Solvate
Formula	C ₂₂ H ₂₀ O ₇	C ₂₂ H ₂₀ O ₇	C ₂₂ H ₁₈ O ₇	C ₂₂ H ₂₀ O ₇ ·MeCN
M _r	396.4	396.4	394.4	437.5
Space group	C2/c	P2 ₁ 2 ₁ 2	P2 ₁ /c	Pbca
a/Å	15.507(3)	4.871(2)	13.546(6)	31.634(6)
b/Å	8.936(1)	27.09(1)	8.141(8)	7.971(3)
c/Å	14.266(4)	7.268(3)	17.18(1)	17.430(8)
β/°	109.66(2)	—	101.05(6)	—
U/Å ³	1 861.7	959.2	1 859.3	4 395.1
Z	4	2	4	8
D _c /g cm ⁻³	1.41	1.37	1.41	1.32
F(000)	832	416	824	1 840
μ(Mo-K _α)/cm ⁻¹	0.64	0.62	—	0.59
Scan range/°	3 ≤ θ ≤ 25	3 ≤ θ ≤ 25	—	3 ≤ θ ≤ 27
h	-18 → 18	0 → 5	—	0 → 40
k	0 → 10	0 → 32	—	0 → 10
l	0 → 16	0 → 8	—	0 → 22
I _{obs.}	1 274	1 001	—	2 048
Cut-off criterion	F < 3σ(F)	F < 1σ(F)	—	F < 2σ(F)
Number of parameters	174	152	—	290
Maximum Δp/σ	0.005	0.05	—	0.05
Res. density/e Å ⁻³	0.3	0.24	—	0.03
R	0.05	0.10	—	0.07
R _w	0.04	0.07	—	—

Table 3. Fractional co-ordinates (× 10⁴) for compound (5)

	x	y	z
O(1)	-5 000	0	6 837(15)
O(2)	-2 357(26)	645(4)	6 520(11)
O(3)	4 755(12)	1 920(2)	1 106(8)
O(4)	1 888(13)	1 945(2)	4 086(9)
C(1)	-3 656(30)	354(5)	5 781(16)
C(2)	-4 112(17)	201(3)	3 843(12)
C(3)	-2 784(17)	390(3)	2 346(13)
C(4)	-870(22)	787(3)	2 101(12)
C(9)	875(23)	795(4)	516(13)
C(8)	2 800(17)	1 141(3)	119(13)
C(7)	3 043(20)	1 533(3)	1 373(14)
C(11)	6 394(18)	1 931(4)	-542(14)
C(6)	1 458(21)	1 556(4)	2 969(13)
C(10)	190(24)	1 993(4)	5 656(13)
C(5)	-391(17)	1 182(3)	3 332(14)

Table 4. Fractional co-ordinates (× 10⁴) for compound (6)

	x	y	z
O(1)	5 000	10 728(3)	2 500
O(2)	6 460(1)	10 383(2)	3 466(2)
O(3)	4 068(1)	2 844(2)	3 659(1)
O(4)	5 438(1)	1 618(2)	4 963(2)
C(1)	5 740(2)	9 830(3)	3 015(2)
C(2)	5 444(2)	8 256(3)	2 897(2)
C(3)	5 945(2)	7 298(3)	3 604(2)
C(4)	5 793(2)	5 808(3)	3 911(2)
C(5)	4 949(2)	5 051(3)	3 563(2)
C(6)	4 854(2)	3 664(3)	3 928(2)
C(7)	5 608(2)	2 978(3)	4 655(2)
C(8)	6 433(2)	3 716(3)	4 994(2)
C(9)	6 518(2)	5 117(3)	4 636(2)
C(10)	3 308(2)	3 394(5)	2 855(3)
C(11)	6 168(3)	892(5)	5 726(3)

solution in acetone. Diffraction quality crystals were readily selected. Fulgide (5) crystallized in well formed orange plates or flat needles of good quality in ordinary light but showing extensive polycrystalline domain structure in polarized light

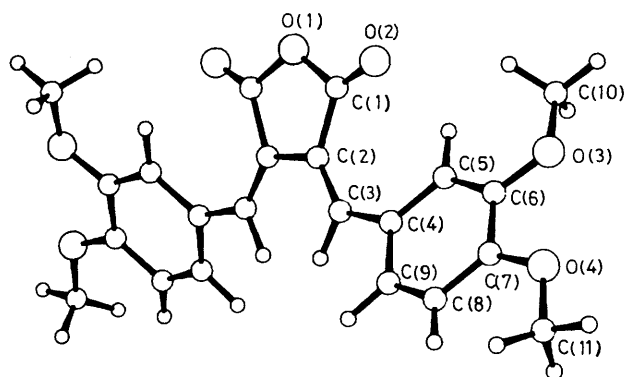
and by X-ray diffraction. Isolated crystals, suitable for crystallographic work, could be selected on two occasions from recrystallized material. Both crystals were found to correspond to the Z,Z-isomer (5). Crystals of (8) were obtained as small but well developed platelets by dissolving it (1 mg) in acetonitrile (100 μl) and dimethylformamide (2 μl) in a sealed tube¹⁶ (45 × 6 mm), briefly heating it to 200 °C, and then keeping it for 17 days while subjecting it to cycles of warming to 80 °C followed by slow cooling. The crystals were of relatively low quality, suitable for crystallographic characterization, but not for detailed refinement. The identity of polycrystalline (5) and single crystals thereof was established by X-ray powder diffraction. The structure of rotamer (9) was obtained by molecular mechanics calculation, using the program of Boyd¹⁷ on a CDC Cyber 750 computer. Another unsymmetrical modification, (10), was indicated by similar calculations. Single crystals of (6) obtained from acetonitrile were shown crystallographically to be solvated.

Crystallographic Analysis.—Crystal data and details of the single-crystal analyses of compounds (5), (6), and (8) and solvated (6) are given in Table 2. All measurements were made on a Nonius CAD4 single-crystal diffractometer with an incident beam graphite-crystal monochromator [$\lambda(\text{Mo-K}_\alpha)$ 0.7107 Å]. The cell constants were determined by least-squares refinement, based on 25 accurately measured 2θ values in the region 16° < θ < 18°. A variable scan speed in ω-2θ mode, adjusted in terms of the intensity during pre-scan, but not exceeding 5.5 ° min⁻¹ and not less than 1 min per reflection, was used for all intensity measurements. Background counting times were adjusted accordingly. The scan width for each reflection was calculated as ω = (0.6 + 0.34 tan θ). The vertical aperture was set at 4.0 mm and the horizontal varied according to the scan width, in the range 1.3–5.9 mm. Intensity checks on three standard reflections were performed each hour to monitor crystal decomposition. None was detected.

Data reduction consisted of correction for background, Lp, and absorption. Absorption corrections were determined empirically¹⁸ from suitable azimuthal scans of nine independent reflections. The structures were solved by direct methods and refined by full-matrix least-squares, using the program¹⁹

Table 5. Fractional co-ordinates ($\times 10^4$) for solvated compound (6)

	x	y	z
O(1)	-450(1)	-3 126(6)	6 966(3)
O(2)	-202(2)	-1 588(7)	7 947(2)
O(3)	1 747(1)	-3 660(6)	5 416(2)
O(4)	2 306(2)	-2 517(6)	6 342(2)
O(2')	-538(2)	-4 426(6)	5 831(3)
O(3')	1 224(1)	2 184(5)	5 324(2)
O(4')	1 364(1)	1 764(6)	3 885(2)
C(1)	-142(2)	-2 172(9)	7 319(4)
C(2)	232(2)	-2 067(7)	6 807(3)
C(3)	598(2)	-1 775(6)	7 150(3)
C(4)	1 033(2)	-1 945(7)	6 914(3)
C(5)	1 349(2)	-1 372(7)	7 417(3)
C(6)	1 774(2)	-1 523(8)	7 241(3)
C(7)	1 900(2)	-2 295(8)	6 570(3)
C(8)	1 585(2)	-2 907(7)	6 059(3)
C(9)	1 164(2)	-2 765(7)	6 230(3)
C(10)	1 466(2)	-3 940(8)	4 777(3)
C(11)	2 634(2)	-1 889(10)	6 824(4)
C(1')	-328(2)	-3 540(8)	6 217(4)
C(2')	77(2)	-2 666(7)	6 051(3)
C(3')	170(2)	-2 370(7)	5 303(3)
C(4')	468(2)	-1 260(7)	4 945(3)
C(5')	538(2)	-1 398(7)	4 150(3)
C(6')	828(2)	-415(7)	3 777(3)
C(7')	1 062(2)	746(8)	4 185(3)
C(8')	987(2)	973(7)	4 988(3)
C(9')	692(2)	-26(6)	5 346(3)
C(10')	1 147(2)	2 530(9)	6 111(3)
C(11')	1 466(2)	1 564(11)	3 082(3)
C(1'')	2 391(3)	-171(12)	4 131(5)
C(2'')	2 225(3)	477(11)	4 850(4)
N	2 519(4)	-671(12)	3 578(4)

**Figure 1.** Atomic numbering schemes for non-hydrogen atoms. Hydrogen atom numbering follows the carbon atom numbers

SHELX, and a weighting scheme based on counting statistics, $R_w = \sum \sqrt{(w|\Delta F|)} / \sum (w|F_o|)$.

Structure (8), by all criteria, did not refine as well as the others, because of the poorer quality crystal, but converged convincingly to an arrangement, completely commensurate with other evidence, to establish firmly the molecular structure. The refined fractional co-ordinates are in Tables 3–5, according to the atomic numbering schemes in Figure 1. Hydrogen atomic numbering follows the numbering of their associated heavy atoms.*

* *Supplementary data* (see section 5.6.3 of Instructions for Authors, in the January issue). Lists of bond lengths and angles, thermal parameters, and H-atom co-ordinates have been deposited at the Cambridge Crystallographic Data centre.

Table 6. Details of the force-field: force constants $k/\text{mdyne } \text{\AA}^{-1}$ or $\text{mdyne } \text{\AA} \text{ rad}^{-1}$ and characteristic, strain-free parameters for bond ($r_0/\text{\AA}$) or angle θ_0/deg) distortions

Bond or angle	k	r_0 or θ_0
C–O(fur)	4.40	1.39
C=O	7.65	1.19
C(1)–C(2)	4.40	1.47
C(3)–C(4)	4.40	1.45
C(2)–C(3)	6.85	1.35
C–C(arom.)	7.65	1.40
C–O(Me)	4.40	1.35
O–C(Me)	4.40	1.43
H–C	5.00	1.08
R–C(sp^3)–R'	0.62	109.5
R–C(sp^2)–R'	0.62	120
C–O–C	0.80	109.5
C–O–C(Me)	0.80	120
C–C–C(arom.)	1.00	120
C(2)–C(2')–C(3)	0.62	130
C(1)–C(2)–C(3)	0.62	116
C(2)–C(3)–C(4)	0.62	128

To establish the identity of the selected single crystal from recrystallized (5) and the bulk material, a powder diffraction pattern was generated by computer methods²⁰ from the single-crystal structure for comparison with the observed powder pattern of bulk (5). The observed pattern recorded on a Rigaku diffractometer, using Cu- K_α radiation, agreed in detail with the calculated, confirming the identities of the single-crystal and bulk materials.

Molecular Mechanics.—Crystallization of the *E,E*-isomer invariably affords compound (6) although n.m.r. analysis indicates the existence in solution of another symmetrical rotamer like (9) accessible by rotation around single bonds which was monitored by molecular mechanics. The reliability of molecular mechanics predictions of configurations depends on the relevance of the force-field, rather than its theoretical basis. A force-field defined from first chemical principles could thus be less appropriate than an empirical force-field adapted to the same type of structure. In the present application an empirical force-field was parametrized against the criterion of correctly predicting the crystallographic structure of (6). However, trial values of harmonic force constants and strain-free bond parameters (k, p_0) were adapted within chemical reason and should be relevant to the interpretation of electronic bond orders.²¹ Numerical detail of the force-field is in Table 6. Currently accepted non-bonded potentials were used without modification.

Free rotations that could produce different rotamers of (6) are possible around carbon bonds C(3)–C(4) and C(3')–C(4') only. Whereas these rotations do not preserve the two-fold symmetry of (6), a limited rotation or flipping around C(2)–C(2') does. It is noted that symmetrical rotamers obtained by the C(2)–C(2') flip are also accessible by rotations around both C(3)–C(4) and C(3')–C(4'), but compared to the C(2)–C(2') flip this latter is less convenient for the sampling of all symmetrical forms. The configurational flip with conservation of symmetry requires simultaneous rotations around the bonds C(3)–C(4), C(2)–C(2'), and C(3')–C(4'). The corresponding torsion angles in the observed structure are -10° , -40° , and -10° , respectively. If it flips to an enantiometric arrangement at 10° , 40° , 10° , over a transition state of -90° , 0° , -90° , rotations of -160° , 80° , and -160° , respectively, are involved. The first rotation should therefore be driven at twice the rate of the second and in an opposite sense.

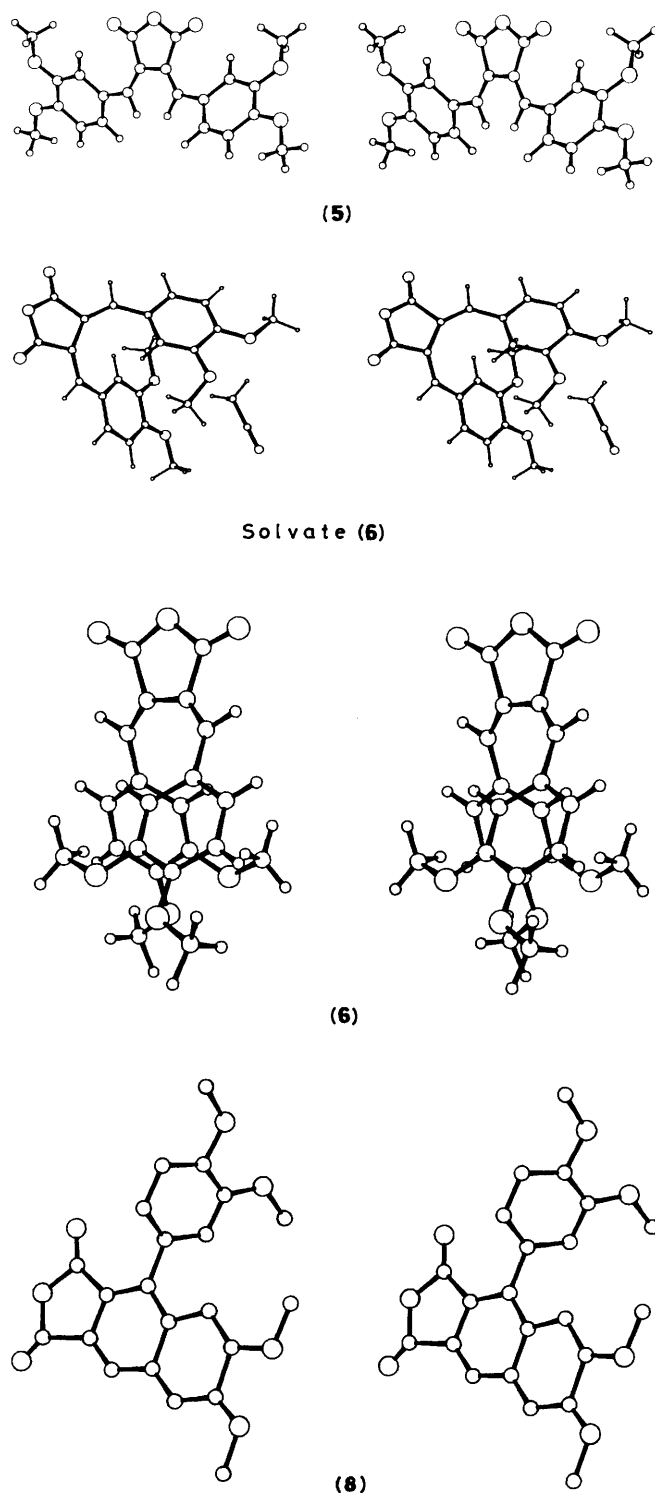


Figure 2. Stereoscopic drawings illustrating the three-dimensional molecular structures of (6), (5), and (8) as obtained crystallographically

Symmetrical (5), *Z,Z* and unsymmetrical [precursor to (8)] *E,Z* open structures arise from forced rotations around C(2)=C(3) double bonds. These rotations have not been examined by molecular mechanics. Barriers to single-bond rotation were calculated by replacing the standard torsional parameter by an artificial incremental parameter¹⁷ to drive the rotation around the bond, sampling the equilibrium steric strain at each position.

Table 7. Comparison of the anhydride configurations in the *X*-ray structures of (6), (5), and (8). The angles ϕ are endocyclic torsion angles in degrees. χ and Q represent puckering mode and amplitude in degrees and \bar{A} , respectively

Compound	(6)	(5)	(8)
$\phi[\text{O}(1)-\text{C}(1)]$	-4.8	-1.1	-2.2
$\phi[\text{C}(1)-\text{C}(2)]$	12.4	2.5	5.7
$\phi[\text{C}(2)-\text{C}(2')]$	-14.6	-3.0	-1.6
χ	90.0	90.0	94.8
Q	0.14	0.06	0.03
Conformation	$\frac{3}{2}T$	$\frac{3}{2}T$	$\frac{3}{2}T$

Results and Discussion

Crystallographic and molecular mechanics results established the number of possible rotamers as five, *viz.* three symmetrical and two unsymmetrical forms. The unsymmetrical open form, however, is unstable and readily dehydrogenates to form a naphthalene structure.

X-Ray Structures.—Two of the symmetrical forms were studied in detail by *X*-ray diffraction. In both structures, (5) and (6), a two-fold axis, through O(1) and bisecting C(2)–C(2'), relates the two halves of the molecule. In addition, the dehydrogenation product (8) of the unsymmetrical open form has also been studied.

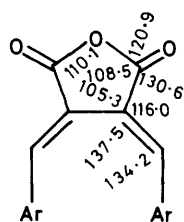
Stereoscopic drawings of the three *X*-ray structures of (5), (6), and (8) are shown in Figure 2. Comparison of the anhydride conformations in the three forms provides an interesting measure of the relative steric strain for each case. A comparison, both in terms of puckering parameters²² and endocyclic torsion angles, is made in Table 7. It clearly indicates (6) as the sterically most strained form. The strain originates from eclipsing of the aryl rings. In the *Z,Z*-form (5) the non-bonded repulsion is eliminated by separation of the rings and in (8) by the formation of a naphthalene structure. The observed difference in density of the two forms probably relates to the eclipsed and open nature of structures (6) and (5), respectively.

The molecular structures of the two crystalline modifications of (6) correspond in detail. The major difference between the solvated and unsolvated forms is the lack of crystallographic symmetry for the former, compared with a molecular two-fold axis in the latter. Most molecular parameters are therefore sampled three times in the two structure analyses. The independent measurements of important parameters are compared in Table 8. The two sets for the solvate are related by a non-crystallographic two-fold axis.

The force-field simulation of (6) is also examined in Table 8. The conformationally important parameters agree well with the observed, the only important differences occurring in the anhydride ring and the methoxy groups. The simulated anhydride ring is somewhat less puckered than the observed. The largest discrepancy is in the endocyclic torsion angle at the central bond, observed as -15.5 and simulated at -2.6° . The conformational type of the two forms however is the same. The methoxy groups are observed and simulated in the aromatic plane. The striking difference of observed C–C–O angles on opposite sides of the C–O bond is not correctly simulated. This reflects a definite electronic effect not accounted for by the force-field. This difference between inner and outer methoxy angles appears to be a general feature^{23,24} of methoxy groups coplanar with aromatic rings because of conjugation between the substituent *p*-type lone-pair orbital and the aromatic system. The orientation of the methoxy methyl groups is not modelled well at all due, in part, to the variability of the observed

Table 8. Comparison of parameters in compounds (6) and solvate (6)

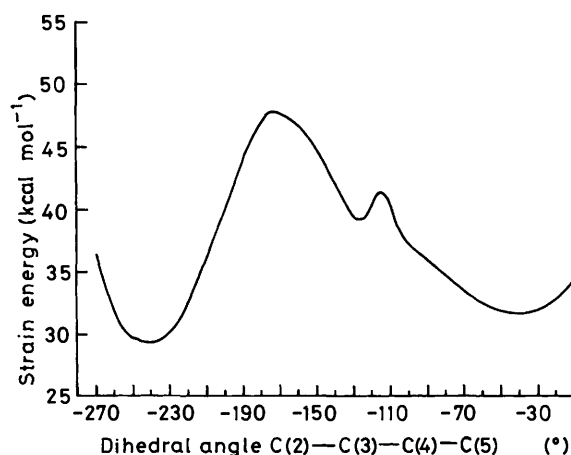
Parameter	Unsolvated (6)	Solvated form		MM
		Unique set	Related set	
O(1)-C(1)	1.39	1.40	1.38	1.40
O(2)-C(1)	1.19	1.18	1.20	1.20
C(1)-C(2)	1.47	1.49	1.48	1.48
C(2)-C(2')	1.46	1.48	—	1.46
C(2)-C(3)	1.35	1.36	1.32	1.36
C(3)-C(4)	1.45	1.44	1.44	1.46
Av (C-C) arom.	1.39	1.39	1.40	1.41
Av (C-O) meth.	1.36	1.36	1.37	1.37
Av (O-CH ₃)	1.44	1.44	1.43	1.44
C(1')-O-C(1)	109.5	110.5	—	110.2
O(1)-C(1)-O(2)	120.2	121.2	120.6	122.3
O(1)-C(1)-C(2)	108.8	108.0	109.0	108.4
O(2)-C(1)-C(2)	131.1	130.9	130.4	129.2
C(1)-C(2)-C(2')	105.4	105.2	104.6	106.3
C(1)-C(2)-C(3)	116.2	117.1	115.8	118.6
C(2')-C(2)-C(3)	137.3	136.5	138.3	132.7
C(2)-C(3)-C(4)	134.3	131.8	133.6	129.1
C(3)-C(4)-C(5)	124.3	123.3	124.1	123.0
C(3)-C(4)-C(9)	117.5	118.9	118.0	117.8
Av (C-C-C) arom.	120.0	120.0	120.0	120.0
Av (O-C-C) outer	125.4	125.9	125.4	119.8
Av (O-C-C) inner	114.9	114.8	114.7	121.0
Av (C-O-C) meth.	117.5	117.6	118.1	122.3
C(1')-O(1)-C(1)-C(2)	-4.9	-4.9	-5.9	-2.2
O(1)-C(1)-C(2)-C(2')	12.7	13.4	14.0	3.0
O(2)-C(1)-C(2)-C(3)	21.5	23.0	24.1	15.0
C(1)-C(2)-C(2')-C(1')	-15.1	-16.2	—	-2.6
C(3')-C(2')-C(2)-C(3)	-42.0	-44.5	—	-41.7
C(2')-C(2)-C(3)-C(4)	-2.6	-1.7	0.0	-2.7
C(2)-C(3)-C(4)-C(5)	-8.7	-9.8	-10.1	-15.4
O-C-C-O	0.0	0.0	1.1	-0.6
C(8)-C(7)-O(4)-C(11)	1.8	-4.0	-0.9	-15.4
C(5)-C(6)-O(3)-C(10)	7.3	-3.4	17.1	-16.7

**Figure 3.** Summary of observed bond angles around the five-membered ring of (6)

C-C-O-C torsion angles. This is probably due to reorientations sensitive to packing energy.

The aryl rings in (6) are not parallel, having their plane normals inclined at an angle of 50°. No unusual bond lengths were observed, but the bond angles at the olefinic trigonal carbon atoms, as shown in Figure 3, are noteworthy. In order to keep C(1)-C(2)-C(2') close to the 108° required for a planar pentagon, the external angle C(2')-C(2)-C(3) opens up to 137°. For the same reason the angle O(2)-C(1)-C(2) is found to be 131°. The opening of C(2)-C(3)-C(4) to 134° occurs for less obvious reasons. It is noted that the reason why the bonds O(2)=C(1) and C(3)=C(2) do not bisect the external ring angles is not entirely of steric origin.

Simulated Structures.—The empirical force-field adapted to reproduce structure (6) was assumed to be appropriate for all rotamers of this compound and for modelling barriers to rotation. Steric energy as a function of an aryl ring rotation is

**Figure 4.** Steric energy of (6) as a function of the rotation of an aryl ring. The potential barrier represents the transition from (6) to (10)

shown in Figure 4. A barrier of about 64 kJ mol⁻¹ separates (6) from an energetically almost equivalent but unsymmetrical form (10), reached after rotation through 180°. This structure, shown stereoscopically in Figure 5, has not been observed in the course of these experiments. This is interpreted to indicate that rotation is restricted by this barrier in the experimental temperature range and that the integrity of the five-membered ring may not be affected in the chromatography step.

The only other possible rotation is around the central bond,

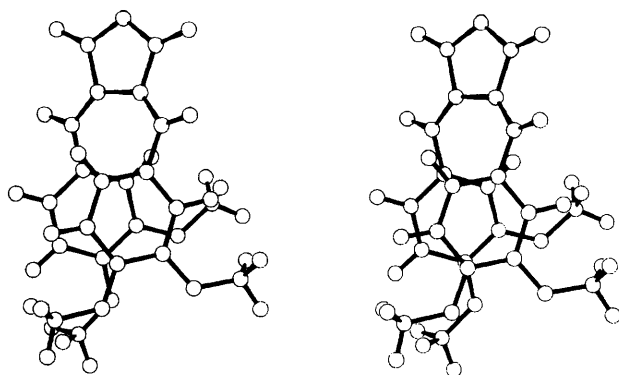


Figure 5. Stereoscopic drawings of the structure (10), obtained by rotation of an aryl ring in (6) by 180°

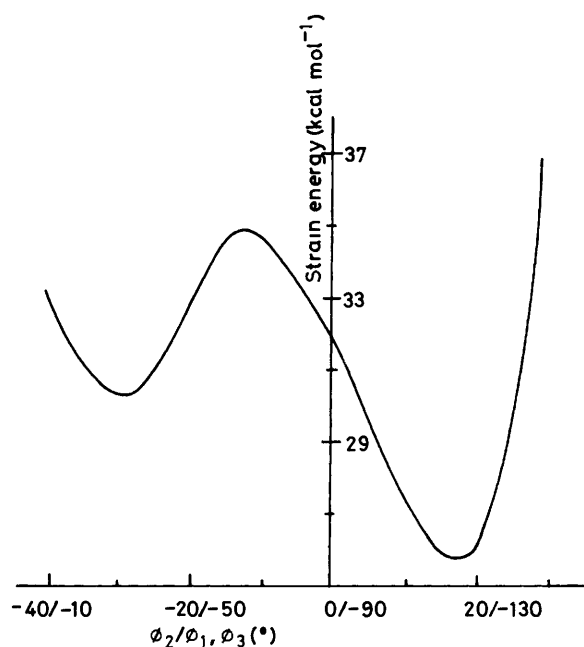


Figure 6. Steric energy profile of rotation around the central C(2)-C(2') bond in (6), coupled with appropriate relaxation through rotations around the C(3)-C(4) bonds

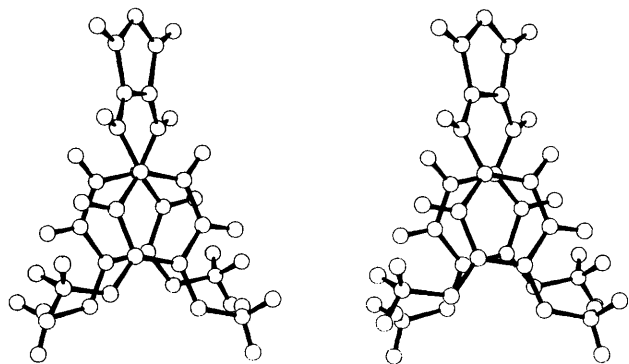


Figure 7. Stereoscopic drawing of structure (9) as obtained by molecular mechanics calculation consisting of limited rotation or flip around C(2)-C(2') starting from structure (6)

Table 9. Calculated orthogonalized atomic co-ordinates for compound (9)

	<i>x</i>	<i>y</i>	<i>z</i>
O(1)	6.554 18	9.586 54	3.358 80
O(2)	4.676 82	9.236 75	2.101 40
O(3)	3.631 42	1.739 77	2.581 94
O(4)	4.847 93	1.243 96	5.088 06
O(2')	8.402 76	9.236 86	4.656 64
O(3')	9.130 58	1.666 06	4.476 23
O(4')	7.885 33	1.120 66	1.995 59
C(1)	5.605 71	8.784 41	2.704 97
C(2)	5.936 03	7.369 37	2.976 65
C(3)	4.994 20	6.406 52	2.775 67
C(4)	4.874 34	5.114 59	3.445 45
C(5)	4.245 25	4.063 33	2.762 27
C(6)	4.220 59	2.756 49	3.291 56
C(7)	4.830 12	2.504 91	4.545 94
C(8)	5.437 87	3.570 92	5.236 72
C(9)	5.458 75	4.861 74	4.694 38
C(10)	3.028 92	1.950 49	1.291 04
C(11)	5.472 49	0.955 68	6.353 70
C(1')	7.475 64	8.784 09	4.050 72
C(2')	7.124 74	7.367 46	3.811 67
C(3')	8.034 22	6.385 03	4.062 93
C(4')	8.086 73	5.061 49	3.448 61
C(5')	8.654 97	4.009 66	4.182 04
C(6')	8.603 32	2.679 88	3.715 82
C(7')	7.979 67	2.404 23	2.473 48
C(8')	7.439 35	3.470 36	1.728 78
C(9')	7.498 82	4.785 45	2.206 18
C(10')	9.739 36	1.904 43	5.759 23
C(11')	7.246 26	0.812 24	0.746 83
H(3)	4.031 53	6.723 01	2.407 36
H(5)	3.825 49	4.271 15	1.790 61
H(8)	5.919 31	3.418 86	6.190 34
H(9)	5.956 10	5.643 81	5.244 32
H(101)	3.699 59	2.315 52	0.525 71
H(102)	2.206 43	2.651 78	1.276 73
H(103)	2.603 87	1.063 99	0.841 33
H(111)	5.421 13	-0.080 75	6.656 82
H(112)	6.529 83	1.174 45	6.405 93
H(113)	5.054 53	1.480 22	7.201 59
H(3')	8.985 92	6.704 71	4.455 22
H(5')	9.083 88	4.238 27	5.144 94
H(8')	6.950 28	3.301 68	0.781 86
H(9')	7.052 83	5.568 64	1.615 28
H(101')	9.120 13	2.351 15	6.524 50
H(102')	10.610 58	2.543 90	5.733 83
H(103')	10.108 92	1.013 36	6.247 38
H(111')	7.232 67	-0.238 83	0.494 19
H(112')	6.204 58	1.093 69	0.680 56
H(113')	7.696 62	1.267 69	-0.124 18

opposite the furyl oxygen atom. The steric energy profile for this rotation coupled with appropriate rotations around the C(3)-C(4) single bonds is presented in Figure 6. Minimum-energy arrangements are predicted at angles of about -30° and $+20^\circ$ of the torsion angle (3-2-2'-3), with a maximum near -10° . The potential barrier is about 20 kJ mol^{-1} , low enough to allow interconversion between (6) and (9). Cartesian atomic co-ordinates for the simulated structure (9) are in Table 9. It is suggested that a similar interconversion between the unsymmetrical structure and its enantiomer is possible.

The most interesting feature of structure (9) shown stereoscopically in Figure 7 is the nearly equivalent disposition of the methoxy groups, with respect to the eclipsing benzene rings, as illustrated by the perspective drawing in Figure 8. It is of further interest to note that rotamer (9) is calculated to be more stable than (6) by *ca.* 20 kJ mol^{-1} , although only (6) seems to occur in the crystalline state. These two factors are probably related. In

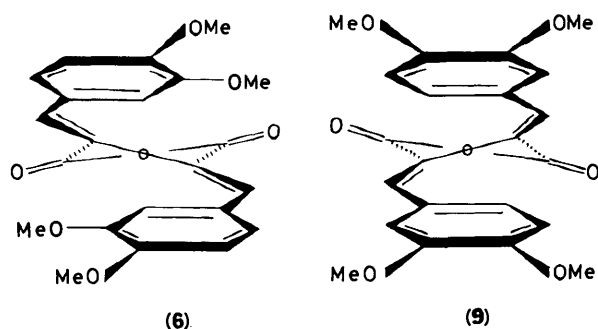


Figure 8. Perspective drawing of stereoisomer (6) and of the stereoisomer (9) generated by flipping (6) about the central bond in the five-membered ring, showing the nearly equivalent disposition of the methoxy groups in (9)

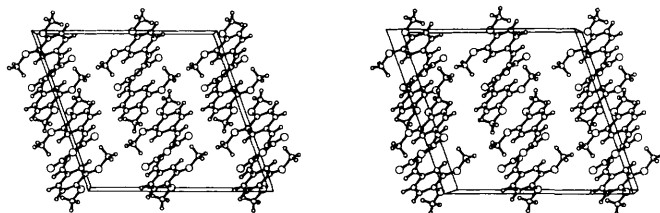


Figure 9. Stereoscopic packing diagram showing the unit cell of (6)

the crystal, neighbouring molecules pack in a head-to-tail fashion with major intermolecular contact between the parallel aryl rings, as shown in the packing diagram of Figure 9. The intermolecular π -interactions benefit from the way in which the methoxy groups lie on the outside of the overlapping aromatic rings. If, because of its different conformation, this efficient mode of packing is not possible between molecules of (9), it could explain why crystals of (6) have the lower lattice energy. The major conformational difference that could affect the packing is in the torsion angles $C(2)-C(3)-C(4)-C(5)$, calculated at *ca.* -30 and -115° for isolated molecules of (6) and (9) respectively. The former represents a flatter type of molecule that should pack together more smoothly than the more angular type of molecule (9), which in turn has its aryl rings more closely in parallel alignment. The major n.m.r. solution signal could therefore quite possibly represent molecule (9), which on crystallization transforms into (6).

Some features of the force-field required for the simulation of the eclipsed structures deserve comment. According to Table 6 accepted values of bond lengths and angles are not adequate everywhere, particularly not around the double bonds to the five-membered ring. Although no adjustment of force constant was attempted during parametrization, the reference values r_0 and θ_0 for bonds in this vicinity clearly indicate extensive delocalization around the conjugated system $C(4)-C(3)-C(2)-C(2')-C(3')-C(4')$ and $O(2)-C(1)-C(2)$ —*etc.* The $O(2)-C(1)-C(2)$ bond angle of 131° , however, results from a simple steric effect. One important consequence of the delocalization would be lowering of the barrier to rotation around the formal double bonds, thus promoting conversion into *E,Z*- and *Z,Z*-isomers. The methoxy groups were modelled to be co-planar with the aromatic rings, as suggested by Anderson *et al.*,²³ and as observed for all the structures reported here, and elsewhere.²⁴

Conclusion

Bis-(3,4-dimethoxybenzylidene)succinic acid forms an anhydride (6) with eclipsed benzene rings related by a molecular two-fold axis. The close eclipsing inhibits free rotation of the

aryl rings by 65 kJ mol^{-1} and unsymmetrical rotamers of (6) have never been identified. The five-membered rings in both simulated structures, (9) and (10), are markedly more planar and the eclipsed aryl rings more parallel, compared with the observed structure, (6). The reason for this becomes obvious on inspection of the different three-dimensional structures. In (6) the *para*-methoxy groups are both directed inwards at each other, whereas all methoxy groups in (9) and (10) are directed away from each other. This allows parallel alignment of the aryl rings and relaxation of the strain in the furyl rings.

The chain, $C(9)-C(4)-C(3)-C(2)-C(2')-C(3')-C(4')-C(9')$ is chiral due to a helical conformation. Compound (6) is formed as a racemic mixture and in the crystal (space group $C2/c$) both left- and right-handed forms are present. The chirality is reversed by flipping about the central $C(2)-C(2')$ single bond in the furan ring across a potential barrier of 20 kJ mol^{-1} . The resulting rotamer (9) is not the enantiomer of (6) since the flipping also changes the relative disposition of the methoxy groups. The pair of rotamers, (6) and (9) can be converted into the enantiomeric pair by 180° rotation of both aryl rings around their connecting single bonds. Rotation of one of the aryl rings only, results in the unsymmetrical eclipsed form that flips into its enantiomer by limited rotation around the central bond, as before. Chirality is lost during forced rotation of an aryl group around a double bond. Rotation of one group produces an unstable *E,Z*-isomer that readily dehydrogenates to form an aromatic ring, by closure of an already extensively delocalized system. Rotation of both groups produces the unstrained open structure of the *Z,Z*-isomer. It is suspected that the formation of unsymmetrical *E,E*-rotamers is prevented by steric factors. This will be the topic of a further study.

Acknowledgements

We thank the foundation for Research Development for comprehensive support, the Council of Scientific and Industrial Research for spectra and computing facilities, Dr. P. R. Boshoff, Mrs. S. Heiss, and Dr. R. J. Highet (N.I.H., Bethesda, MD) for spectra, and Mrs. C. C. Allen and Miss M. D. Madiope for the computer drawings and general assistance.

References

- H. Stobbe, *Justus Liebig's Ann. Chem.*, 1911, **380**, 1.
- H. Stobbe, *Justus Liebig's Ann. Chem.*, 1911, **380**, 17.
- H. Stobbe, *Justus Liebig's Ann. Chem.*, 1908, **359**, 1; cf. H.-D. Ilge and R. Paetzold, *Z. Chem.*, 1983, **23**, 221, and K. Gustav, J. Sühnel, W. Weinrich, and R. Paetzold, *ibid.*, 1979, **19**, 219.
- H. Stobbe, *Ber. Deutsch. Chem. Ges.*, 1907, **40**, 3372; F. G. Baddar, E. H. Ghaly, and M. F. El-Newehy, *J. Chem. Soc.*, 1961, 2528 and references therein.
- H. Stobbe and K. Leuner, *Justus Liebig's Ann. Chem.*, 1911, **380**, 75.
- Particularly by H. G. Heller *et al.*, e.g. O. Crescente, H. G. Heller, and S. Oliver, *J. Chem. Soc., Perkin Trans. 1*, 1979, 150.
- M. D. Cohen, H. W. Kaufman, D. Sinnreich, and G. M. J. Schmidt, *J. Chem. Soc. B*, 1970, 1035.
- J. C. A. Boeyens, L. Denner, and G. W. Perold, *J. Chem. Soc., Perkin Trans. 2*, in the press.
- H. Stobbe and K. Leuner, *Justus Liebig's Ann. Chem.*, 1911, **380**, 75.
- P. R. Boshoff and G. W. Perold, *J. Chem. Res.*, 1986, (S), 80; (M), 0735.
- E. L. Eliel, 'Stereochemistry of Carbon Compounds,' McGraw-Hill, New York, 1962, 330.
- J. C. A. Boeyens, L. Denner, and G. W. Perold, *S. Afr. J. Chem.*, 1987, **40**, 44.
- H. O. House and J. K. Larson, *J. Org. Chem.*, 1968, **33**, 448.
- J. Lebbe, in J. Tranchant (ed.), 'Practical Manual of Gas Chromatography,' Elsevier, London, 1969, 264.
- F. G. Baddar, H. A. Fahim, and M. A. Galaby, *J. Chem. Soc.*, 1955, 465.
- J. C. A. Boeyens, M. U. Naude, and G. W. Perold, *S. Afr. J. Chem.*, 1982, **35**, 157.
- R. H. Boyd, *J. Chem. Phys.*, 1968, **49**, 2574.

- 18 A. C. T. North, D. C. Phillips, and F. S. Mathews, *Acta Crystallogr., Sect. A*, 1968, **24**, 351.
- 19 G. M. Sheldrick in H. Schenk, (ed.), 'Computing in Crystallography', University Press, Delft, 1978.
- 20 K. Yvon, W. Jentschko, and I. Parthé, *J. Appl. Crystallogr.*, 1977, **10**, 73.
- 21 J. C. A. Boeyens, F. A. Cotton, and S. Han, *Inorg. Chem.*, 1985, **24**, 1750.
- 22 D. Cremer and J. A. Pople, *J. Am. Chem. Soc.*, 1975, **97**, 1358.
- 23 G. M. Anderson, P. A. Kollman, L. N. Domelsmith, and K. N. Houk, *J. Am. Chem. Soc.*, 1979, **101**, 2344.
- 24 I. L. Karle, J. L. Flippen-Anderson, J. F. Chiang, and A. H. Lowrey, *Acta Crystallogr., Sect. B*, 1984, **40**, 500.

Received 7th July 1987; Paper 7/1219